

Article

Nonlinear Analyses of Adobe Masonry Walls Reinforced with Fiberglass Mesh

Vincenzo Giamundo, Gian Piero Lignola *, Andrea Prota and Gaetano Manfredi

Department of Structures (Di.St.), University of Naples Federico II, Via Claudio 21, Naples 80125; Italy, E-Mails: vincenzo.giamundo@unina.it (V.G.); aprota@unina.it (A.P.); gamanfre@unina.it (G.M.)

* Author to whom correspondence should be addressed; E-Mail: glignola@unina.it; Tel.: +39-081-768-3492; Fax: +39-081-768-5921.

Received: 5 December 2013; in revised form: 30 January 2014 / Accepted: 10 February 2014 / Published: 17 February 2014

Abstract: Adobe constructions were widespread in the ancient world, and earth was one of the most used construction materials in ancient times. Therefore, the preservation of adobe structures, especially against seismic events, is nowadays an important structural issue. Previous experimental tests have shown that the ratio between mortar and brick mechanical properties (*i.e.*, strength, stiffness and elastic modulus) influences the global response of the walls in terms of strength and ductility. Accurate analyses are presented in both the case of unreinforced and reinforced with fiberglass mesh when varying the mechanical properties of the materials composing the adobe masonry structure. The main issues and variability in the behavior of seismic resisting walls when varying the mechanical properties are herein highlighted. The aim of the overall research activity is to improve the knowledge about the structural behavior of adobe structural members unreinforced and reinforced with fiberglass mesh inside horizontal mortar joints.

Keywords: adobe; fiber reinforced polymer (FRP); masonry walls; fiberglass mesh; finite element method; nonlinear analysis; seismic vulnerability; retrofit

1. Introduction

Earth is one of the oldest and most widespread construction material used in the construction of buildings and has been used for thousands of years. Earth can be considered the cheapest material

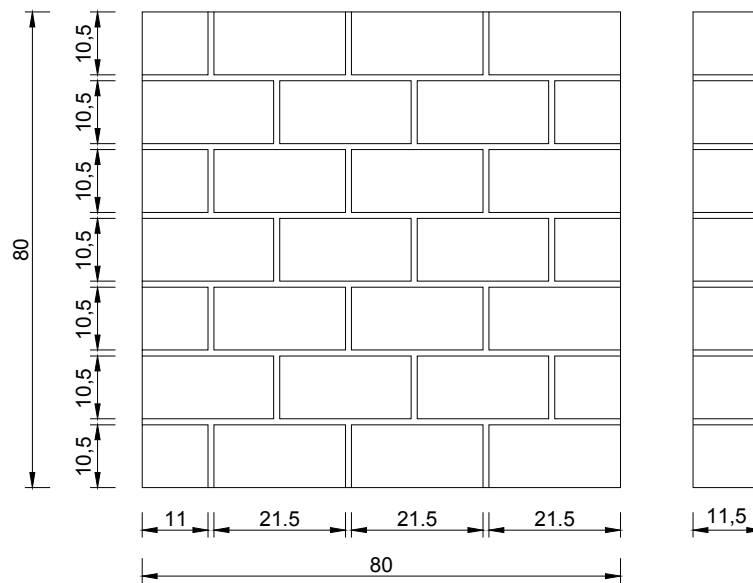
readily available for construction. It has been extensively used for masonry constructions around the world. The popularity of adobe is also related to the low level of skill and technology required for the production of the bricks and construction. Furthermore, due to its inherent properties, earth is an efficient heat and sound insulating material [1,2]. After the introduction of reinforced concrete, the number of adobe buildings has become progressively less. Nevertheless, as reported in [3], it is estimated that approximately 30% of the world's population still lives in buildings made of earth. In spite of its past and present spread, adobe constructions are prone to damage under seismic actions [4], and most of these buildings are located in high seismic risk areas. Therefore, there is nowadays raising awareness for the preservation of historic, archeological, or even still in use structures. Unfortunately research on the structural behavior of adobe buildings, and especially on their reinforcement, is inadequate, so far. The seismic resistance of adobe masonry structures primarily depends on the in-plane shear behavior of individual walls. The typical failure mode under earthquakes is the diagonal cracking mode. This occurs when the principal tensile stresses developed in the wall, under a combination of vertical and horizontal loads, exceed the tensile strength of the adobe material. The seismic characterization of the masonry structural element is generally carried out through direct shear tests or diagonal compression tests. According to [5], the diagonal compression test allows the determination of the diagonal tensile (or shear strength) of masonry assemblages. The test consists in loading the specimen in compression along one diagonal, resulting in a diagonal tension failure. This test allows for the evaluation of the effects of variables, such as the type of masonry unit, mortar, workmanship, *etc.* [6]. The use of plaster reinforcement mesh between adobe blocks, in the construction phase, can significantly improve the shear strength of adobe walls. Fiberglass mesh is a glass fiber fabric, usually coated with a polymer latex-resistant matrix. It is widely used in the building industry as a plaster stiffener or as a wall reinforcement (anti-crack). Previous experimental tests by [7] showed the effect of fiberglass reinforcement on adobe masonry walls. These tests represent the base of the present paper.

2. Summary of Experimental Outcomes

2.1. Test Setup

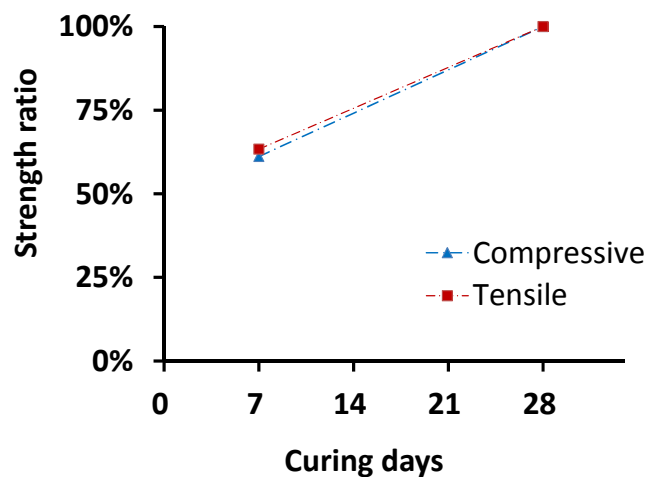
Experimental diagonal compression tests on adobe wall panels (unreinforced and reinforced with plaster fiberglass mesh) presented in [7] have been used as a benchmark for the validation of the herein presented numerical analyses. All the tested panels were subjected to diagonal compressive load (compressive edge load) acting in the plane of the wall and forming a 45° angle with the direction of the mortar bed joints; the geometry of a tested panel is reproduced in Figure 1.

The specimens were built with the global size of $80 \times 80 \text{ cm}^2$. The brick unit size was $11.5 \times 10.5 \times 21.5 \text{ cm}^3$. The mortar thickness was 10 mm, while the width (the third out-of-plane dimension) was 11.5 cm for both bricks and mortar. Different adobe soil curing for both the bricks and the mortar were used for each specimen. The reinforced panels were built placing a plaster reinforcement fiberglass mesh (with equal spacing of $5 \text{ mm} \times 5 \text{ mm}$) inside the horizontal mortar joint of the adobe blocks. This sort of mesh fiber reinforcement is very cheap and commonly used for reinforced plaster coatings, usually applied on the exterior and interior faces of walls by the construction industry.

Figure 1. Tested panel geometry.

2.2. Material Characterization

An essential mechanical characterization of the material is provided in [7]. Nevertheless, further data not present in [7] have been achieved by fitting numerical global experimental data. Tensile and compressive strengths of both the brick and the mortar, at different curing times, were achieved by interpolation according to the values suggested in [8]. Such tests provide data from 0 to 28 days of curing for plain soil. The elastic modulus, E , of the adobe soil was achieved by fitting the global response curve, because such mechanical characterization was lacking. According to the tests presented in [8], the trends of the compressive and tensile strength ratio when varying the curing time are shown in Figure 2. The strength ratio is defined as the ratio between the actual strength (related to the curing time) and the maximum strength. As shown in Figure 2 the compressive strength of the plain soil is almost doubled after about three weeks. Being that both the mortar and the bricks made of the adobe soil, the increase of strength should be considered either for brick and mortar according to their curing time.

Figure 2. Compressive and tensile strength trends when varying the curing time.

3. Nonlinear Numerical Analyses

3.1. Finite Element Method

The influence of the different constituent materials (*i.e.*, the local properties of soil, composition, curing), as well as the fiberglass plaster mesh reinforcement on the global structural behavior has been studied by means of a finite element method (FEM) model. The FEM model has been validated comparing the numerical FEM outcomes to the experimental data [7]. Micromodeling was adopted and some parametric analyses were conducted on validated models. Numerical two-dimensional analyses have been performed. Since the width of the panel is much lower than the other two dimensions, a plane-stress assumption was adopted, and in-plane loads were applied. Different mechanical properties are provided for plain adobe soil when varying the curing time. In particular, the analyses were performed when varying the strength (tensile and compressive) of both, the bricks and the mortar, according to the curing time. In particular, bricks at the testing time [7] were 28 days old, while mortar was almost fresh. Typical values for the fiberglass mesh mechanical parameters have been used. In particular, according to the experimental tests, a fiberglass mesh with the following properties has been considered: weight 100 g/m², density 2.5 g/cm³, elastic modulus 20 GPa and strength 1000 N/50 mm. Lacking an experimental counterpart, for comparison purposes, numerical simulations were performed considering two more cases: the first one applying a mortar having higher performances compared to plain fresh mortar, namely, “mortar B”; the second one considering for both mortar and bricks the same properties, due to the long time of the curing (*i.e.*, longer than 28 days), namely “long-term curing”. The adopted values for the tensile and compressive strength, according to curing time, are reported in Table 1.

Table 1. Material mechanical properties.

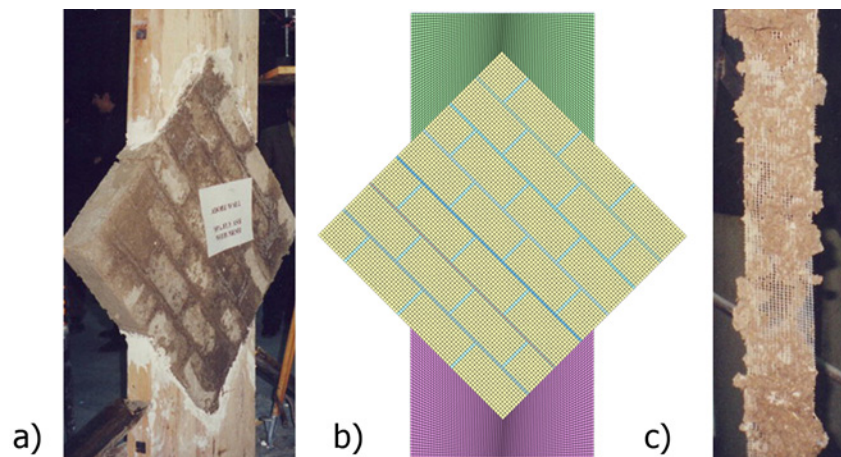
Properties	Fresh plain soil	Plain soil	Plain soil	Mortar B
Curing time (days)	0	28	>28	0
Tensile strength (kPa)	39.2	78.4	98	98
Compressive strength (MPa)	3.32	6.64	8.30	8.30

The FEM model used is constituted of more than 13,000 eight-node quadrilateral isoparametric plane stress elements based on quadratic interpolation and Gauss integration (Figure 3b).

All the analyses have been performed by means of the TNO DIANA v9.4.4 code. In the FEM model, bricks and mortar are modeled individually, without interface elements between them, according to the total strain model coupled with the rotating crack stress-strain relationship approach. In particular, in the total strain approach, the constitutive model describes the stress as a function of the strain. In the rotating crack approach, stress-strain relationships are evaluated in the principal directions of the strain vector, as reported in [9]. Furthermore, the combined Rankine/von Mises yield criterion was adopted. Interface elements have been neglected, according to previous studies [6,10–12], mainly due to the lack of experimental properties. The reinforcement has been modeled as bar reinforcements embedded in all plane stress elements at the horizontal mortar joint locations. In particular, 1D bar reinforcement elements have been used; for these elements, the strains are computed from the displacement field of the mother elements. Thus, a perfect bond between the

reinforcement and the surrounding material is assumed [9]. The total area of the reinforcement grid cross-section has been modeled as the equivalent area concentrated in the reinforcement bar cross-section.

Figure 3. Test setup: (a) experimental; (b) finite element model; and (c) removed fiberglass mesh from the horizontal mortar joint ((a) and (c) were reprinted from [7], Copyright 2001 Elsevier).



Few data were available for constituent materials, especially for the nonlinear post peak phase; therefore, ideal plasticity was assumed in compression. This assumption is acceptable, since the compressive strength has never been reached during the analyses, remarking that the tensile behavior governs the problem. Therefore, in tension, two limit cases were considered, namely “ideal plasticity” and “brittle failure”. The “brittle failure” represents the worst case, which is the more realistic, as well. This case has been modeled by means of an elastic-brittle model. Whereas the “ideal plasticity”, which represents the upper bound, has been modeled by means of an elastic-perfectly plastic model. These two cases have been considered in order to define the boundaries between which the real behavior has to be. All the analyses were performed under displacement control, measuring in-plane deformations and the evolution of reacting stresses. The diagonal compressive axial load has been applied, as a displacement load, through two wooden supports. The supports have been modeled at the two opposite corners of the panel, according to the experimental test setup [7]. Eight-node quadrilateral isoparametric plane stress elements were used to model the supports, as well. As a boundary condition, the bases were fixed.

3.2. Numerical Program

The results of FEM analyses were validated through a comparison between experimental and numerical outcomes. In particular, three main cases were considered, each one including both the tensile plasticity models introduced in the previous section (*i.e.*, ideal plasticity and brittle failure.). Moreover, for each main case, both reinforced and unreinforced wall configurations have been analyzed. The three main cases considered have been named as follows:

- Plain tested: the wall is made of plain adobe bricks, 28 days curing and fresh plain mortar (*i.e.*, 0 day curing), the elastic modulus for both materials is 20 MPa based on experimental data fitting;

- Long-term curing (LTC): this wall, not tested in reality, is made of plain adobe bricks and plain mortar after a long curing time (*i.e.*, a curing time higher than about 28 days); elastic moduli were the same as the first case, for comparison purposes;
- Mortar B (MB): this wall, not tested in reality, is considered only for comparison purposes with the plain tested wall; the wall is made of plain adobe bricks, 28 days curing and a better mortar compared to plain soil; elastic moduli were the same as the first case, for comparison purposes.

The masonry material properties used in the FEM analyses are listed in the following Table 2. The plain soil properties are based on experimental outcomes [7,8]. Conversely, since LTC and MB panels were not tested in reality, their properties are based on the material property trends listed in Table 1. The elastic modulus is derived from best fitting of the global experimental curve for a plain unreinforced panel.

Table 2. Material parameters used for the finite element method (FEM) analyses.
LTC, long-term curing; MB, Mortar B.

FEM model	Brick tensile strength (kPa)	Mortar tensile strength (kPa)	Brick compressive strength (MPa)	Mortar compressive strength (MPa)
Plain	78.4	39.2	6.64	3.32
LTC	98.0	98.0	8.30	8.30
MB	78.4	98.0	6.64	8.3

4. Outcomes of Numerical Analyses

4.1. Experimental Theoretical Comparison

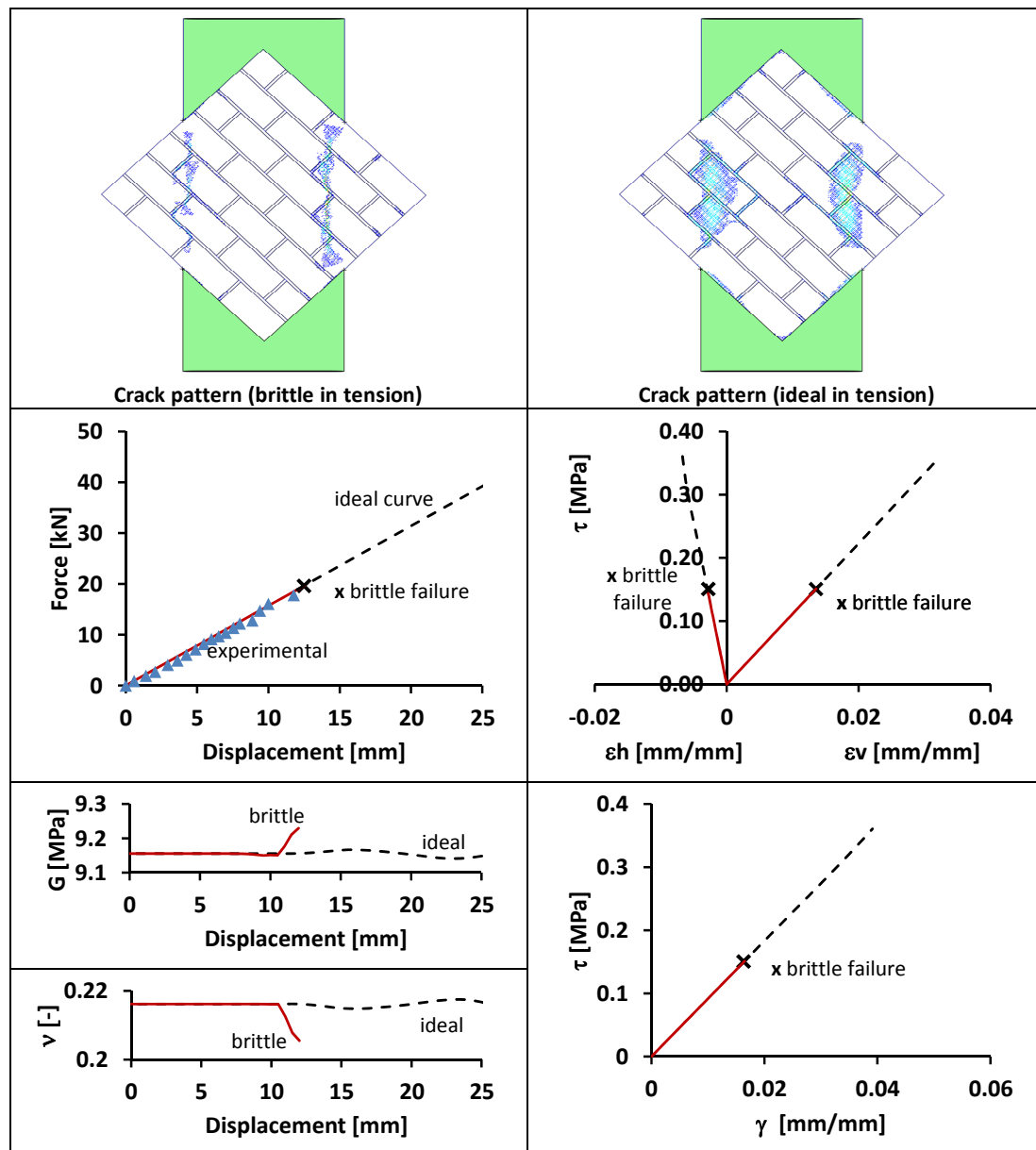
The behavior of adobe wall panels (unreinforced and reinforced with fiberglass mesh) was analyzed (when varying tension softening models) in terms of the force/displacement curve, shear stress-average diagonal strain curve, shear stress-average shear strain curve, Poisson ratio-displacement and Shear modulus-displacement curves. According to [5], for the standard method, the shear stress, τ , has been computed as $\tau = 0.707 \cdot V/A_n$, where V = diagonal load and A_n = the net section area of the uncracked section of the panel (in the considered case, $A_n = 0.092 \text{ m}^2$). The average vertical and horizontal strains, ε_v and ε_h , have been computed as the average displacement along the compressive and tensile diagonals, respectively, over the same gauge length (400 mm). The shear strain, γ , according to [5], is: $\gamma = \varepsilon_v + \varepsilon_h$. The shear modulus, G , and the Poisson ratio, ν , were computed according to the well-known solid mechanics relationships, as $\nu = -\varepsilon_h/\varepsilon_v$ and $G = \tau/\gamma$, respectively. Failure modes, in all the considered cases, were also checked by means of the crack patterns. The experimental failure mode mainly involved the cracking and detachment of lateral corners of the panel, outside the compressed strut between the two wooden loading supports. In the considered cases, the numerical outcomes mainly showed the same cracking pattern, but the spreading of cracks (smeared crack strain field in numerical simulations) depends mainly on the post peak tensile behavior of the soil. In the next figures, solid signs represent experimental data, while continuous and dashed lines represent brittle and ideal post-peak tensile behavior, respectively (*i.e.*, the adopted tensile plasticity model), in FEM outcomes. A small cross marks the failure point for brittle material.

4.2. FEM Models: Validation

The FEM model has been validated both in the cases of unreinforced and reinforced plain panels. In both the cases, mortar and bricks are made of the same material. However, different curing times differentiate the two materials. In particular, the mortar is almost fresh, while bricks are cured for 28 days. Therefore, the strength of the brick is higher in both tension and compression.

The main outcomes of the numerical analyses and a comparison between the numerical and experimental force/displacement curves are presented in Figure 4 in the case of an unreinforced panel.

Figure 4. Experimental-theoretical comparison (unreinforced plain adobe soil).



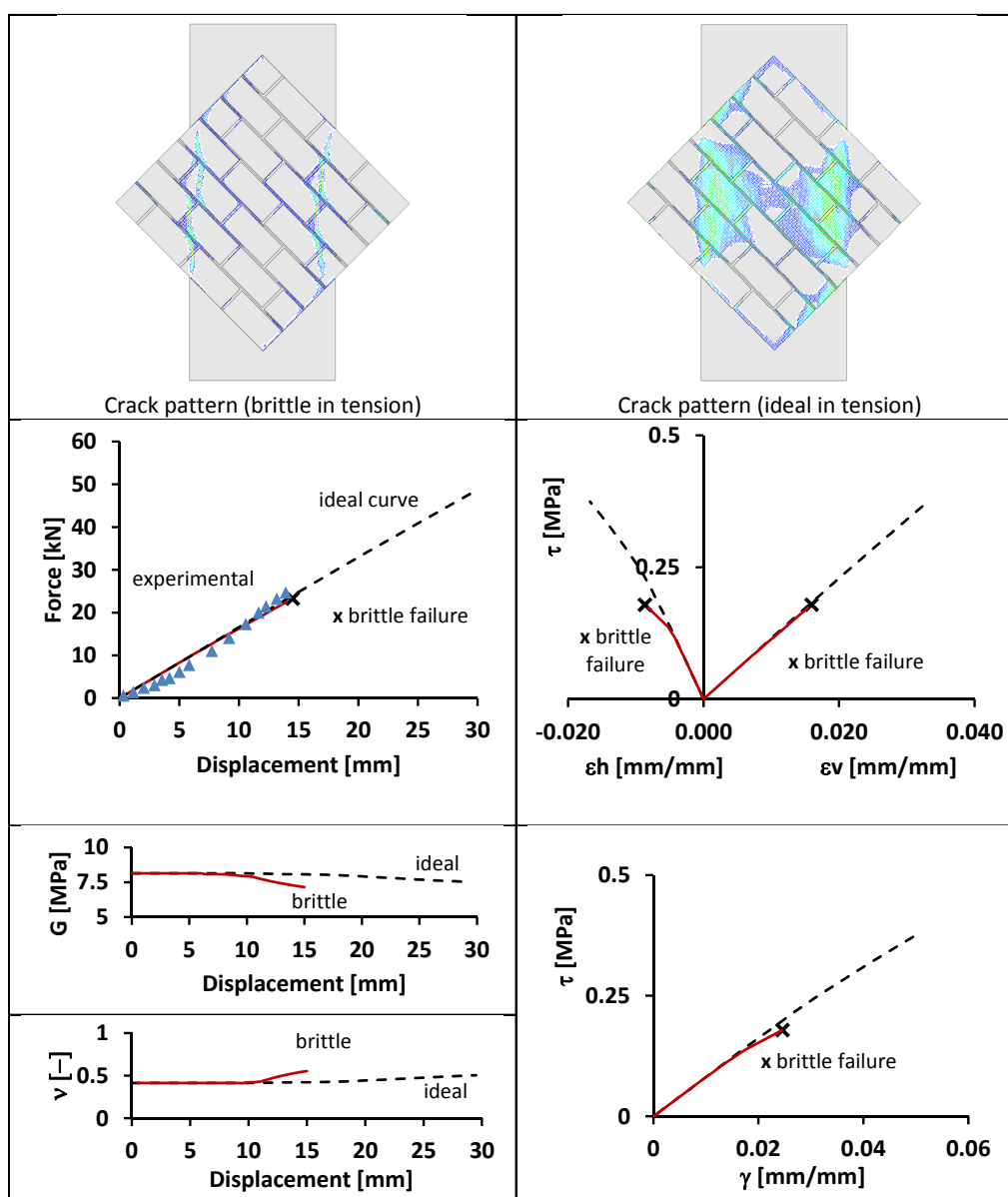
According to the results shown in Figure 4, the brittle material model seems to catch the experimental failure better, in terms of both failure load and the crack pattern. Actually, as shown in Figure 5, the crack pattern is widely smeared, and it almost involves vertical lines connecting the wooden supports.

Figure 5. Detail of the experimental crack pattern (unreinforced plain adobe soil) (reprinted with permission from [7], Copyright 2001 Elsevier).



The global response of the reinforced panel in terms of force/displacement highlights, as well as the unreinforced panel is an almost linear behavior (see Figure 6).

Figure 6. Experimental-theoretical comparison (reinforced plain soil panel).



The brittle material model catches the experimental failure better, both in terms of crack pattern and failure load. In the case of the brittle material, the shear modulus, G , as well as the Poisson ratio, ν , exhibits, up to the failure, the same trend as the case of the ideal material. Of course, the ideal material yields to a longer loading branch. The strength of the plain panel with mesh is about 25% higher, compared to plain soil without mesh, and the ultimate displacement is about 50% higher, so that the benefits of a thin fiber mesh are evident.

4.3. FEM Models: Long-Term Curing (LTC)

The LTC panels were not experimentally tested, but they are analyzed to assess the influence of curing time (*i.e.*, strength) of materials on the global behavior of the masonry panels. Since mortar and bricks have identical mechanical properties, these panels can be considered as practically homogeneous panels. The strengths of the two materials correspond to more than 28 days curing, and it is about 25% higher, compared to plain soil bricks (28 days curing) and 2.5 times higher than plain soil mortar (0 day curing). The global response in terms of force/displacement is almost linear up to the failure point (Figure 7). The shear strength achieved is almost doubled if compared to the first unreinforced plain panel. In any case, the main difference, compared to the first test, is the strength of the materials. The global effect is an increase of the shear strength, being comparable to the increase of the mortar strength. The crack pattern of the unreinforced panel is almost restricted to the vertical lines connecting the wooden supports, but it is quite smeared, due to the higher strength of this panel.

In the case of reinforced LTC panel (Figure 8), the crack pattern achieved is similar to the one achieved in the case of the reinforced plain panel (Figure 6). However, a wider crack pattern was found, due to the higher mechanical properties. The global response in terms of force/displacement is almost linear up to the failure point in the case of the ideal material. However, in the case of brittle material, the graph has a second, less stiff branch after a displacement of 17 mm. The stiffness reduction is related to global cracking damage coupled with a shear modulus, G , drop and the Poisson ratio, ν . The difference, compared to the plain panel with mesh, is the strength of materials, and the global effect is an increase of the shear strength comparable to the increase of the basic material strength (about doubled). Compared to the plain panel without mesh, an increase of strength of about 2.3 times is noticed, while the ultimate displacement is almost doubled.

Figure 7. Numerical experimentation (unreinforced LTC panel).

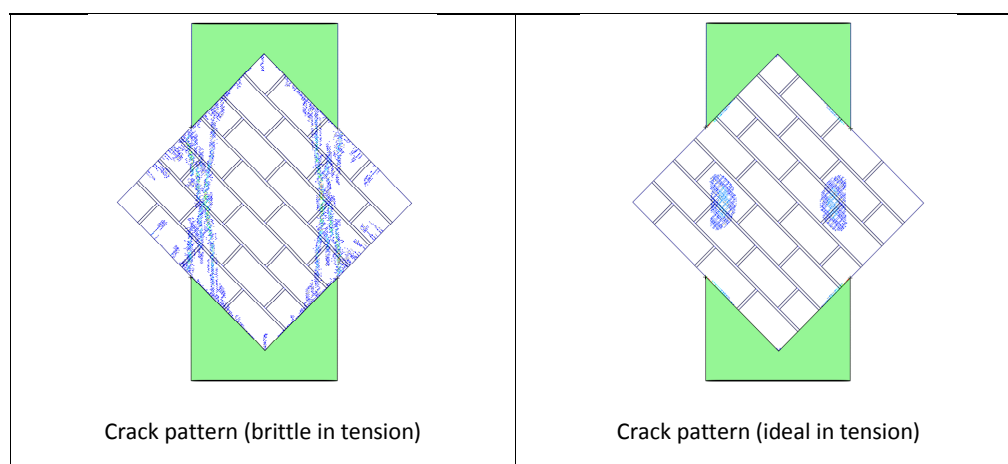


Figure 7. Cont.

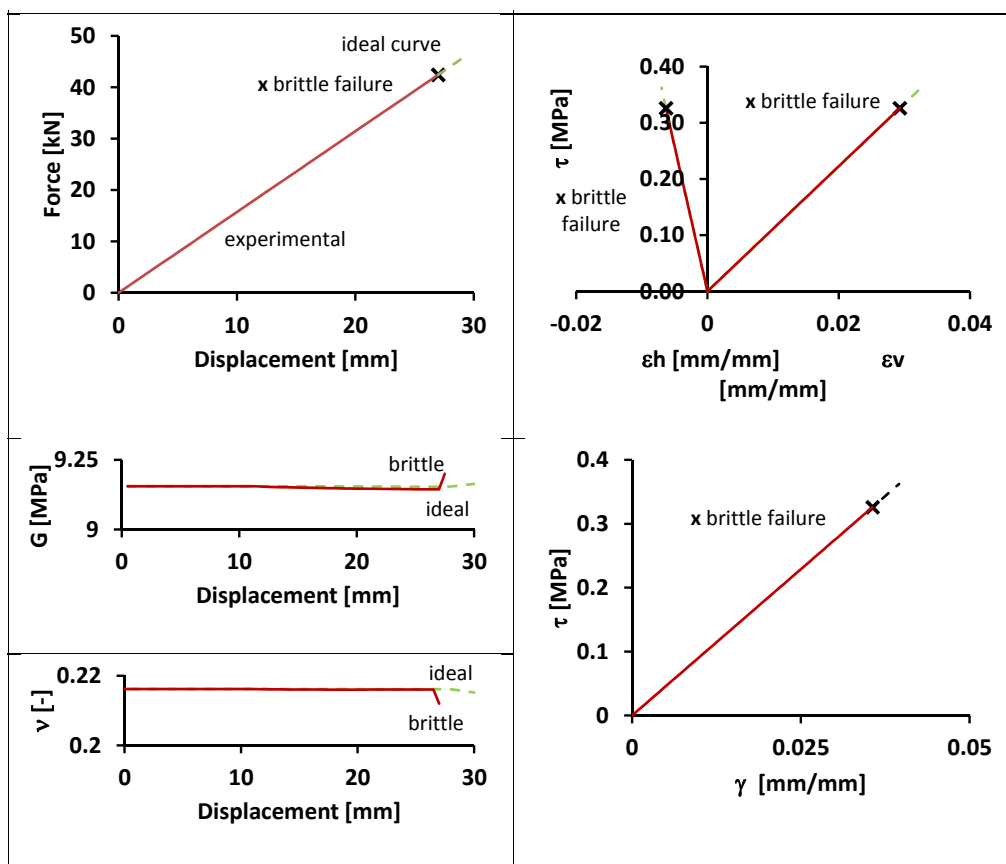


Figure 8. Numerical experimentation (reinforced LTC panel).

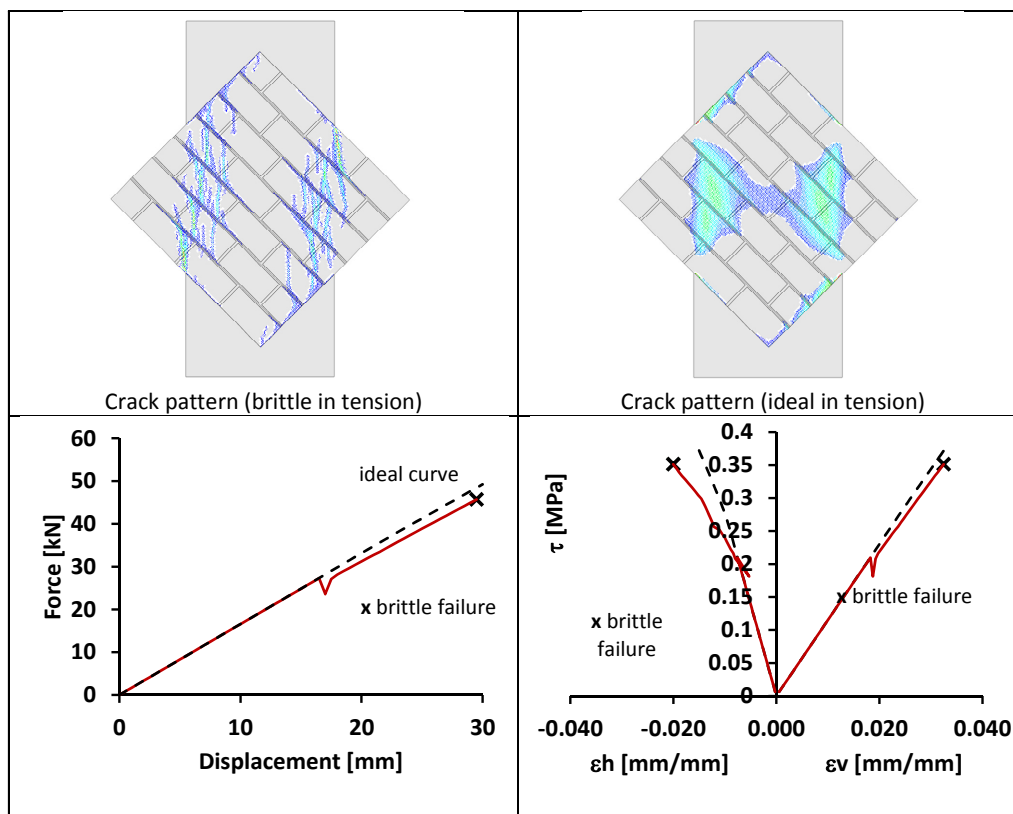
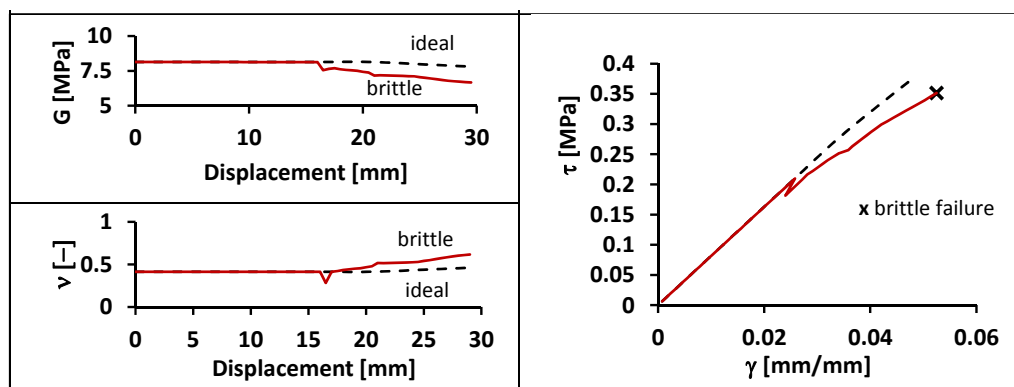


Figure 8. Cont.



4.4. FEM Models: Mortar B (MB)

The panels modeled with a better mortar, as well as the previous LTC panels were not tested in reality. However, this case has been analyzed to assess the influence of the strength of the mortar on the global behavior of the masonry panels. The MB panels are still almost homogeneous panels (having identical elastic moduli). However, the strength of the mortar is about 2.5 times higher, compared to plain soil mortar (0 day curing), while the brick properties are the same as the plain panels case. In the case of the unreinforced panel, both the crack pattern and the global response in terms of force/displacement are almost similar compared to the unreinforced plain panel (Figure 9). Nevertheless, the panel presents a higher ultimate load and shear strength. The comparison with the unreinforced plain panel test allows one to find, in general, a spreading of the crack pattern and higher global performances; however, an easier and more direct comparison can be made with the previous unreinforced long-term curing test. Actually, the main difference, compared to the previous test, is the strength of the brick (that in this case is lower than the previous case), and the global effect is a reduction of the shear strength (almost 20% smaller), being comparable to the reduction of the strength of the bricks.

In the reinforced MB panel, the global response in terms of force/displacement and crack pattern is almost similar to the previous case of the long-term curing panel reinforced with mesh (Figure 10). The main reason for this result is the presence of the mesh reinforcement. Actually, the reinforcement makes less evident the benefits of the strength of the basic materials on the global behavior (and in particular, the properties of the mortar where the mesh reinforcement is placed). As well as in the previous LTC case, compared to the plain panel with mesh, the strength is doubled. Compared to the plain panel without mesh, the increase of strength is about 2.3 times, and the ultimate displacement is doubled.

Figure 9. Numerical experimentation (unreinforced MB panel).

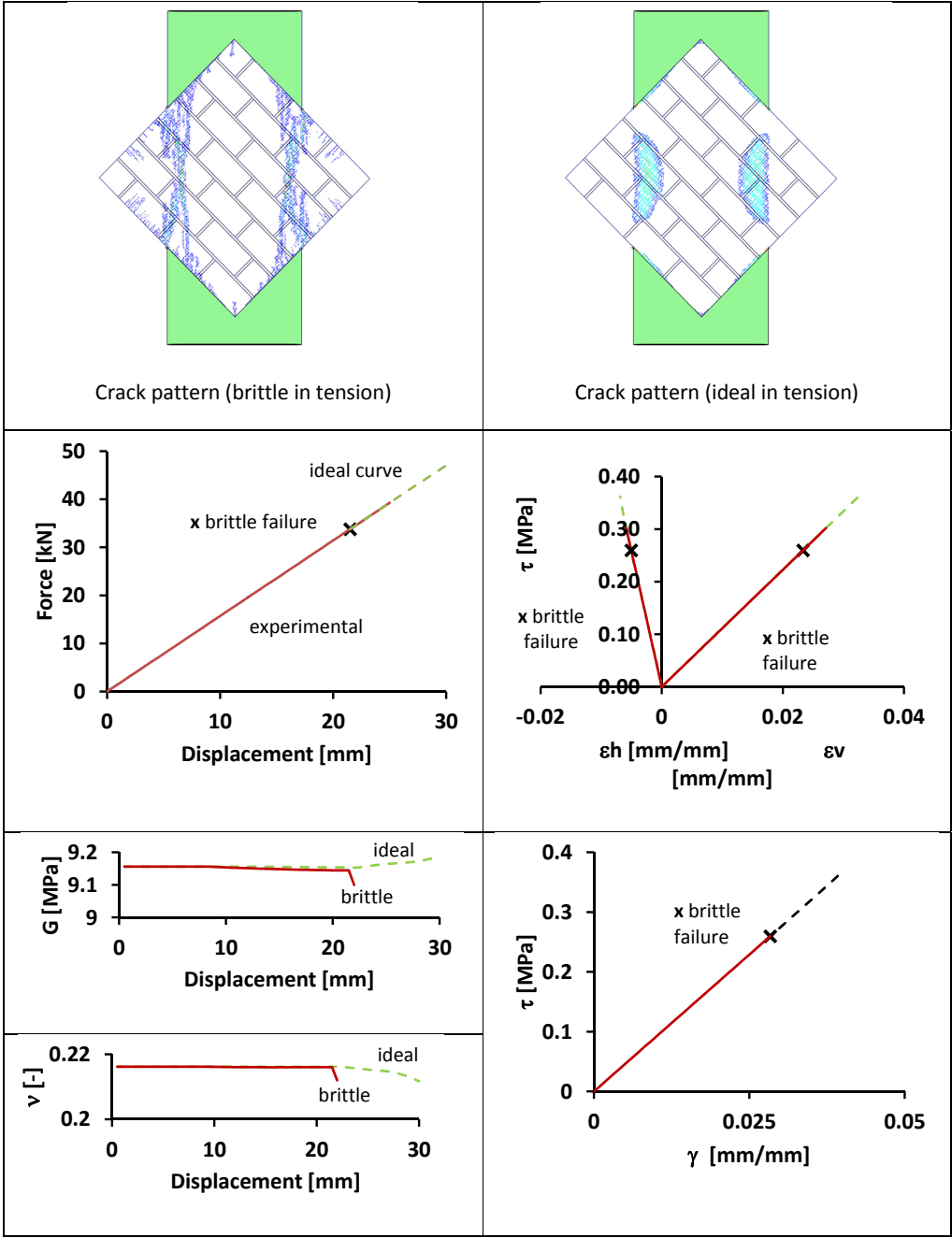
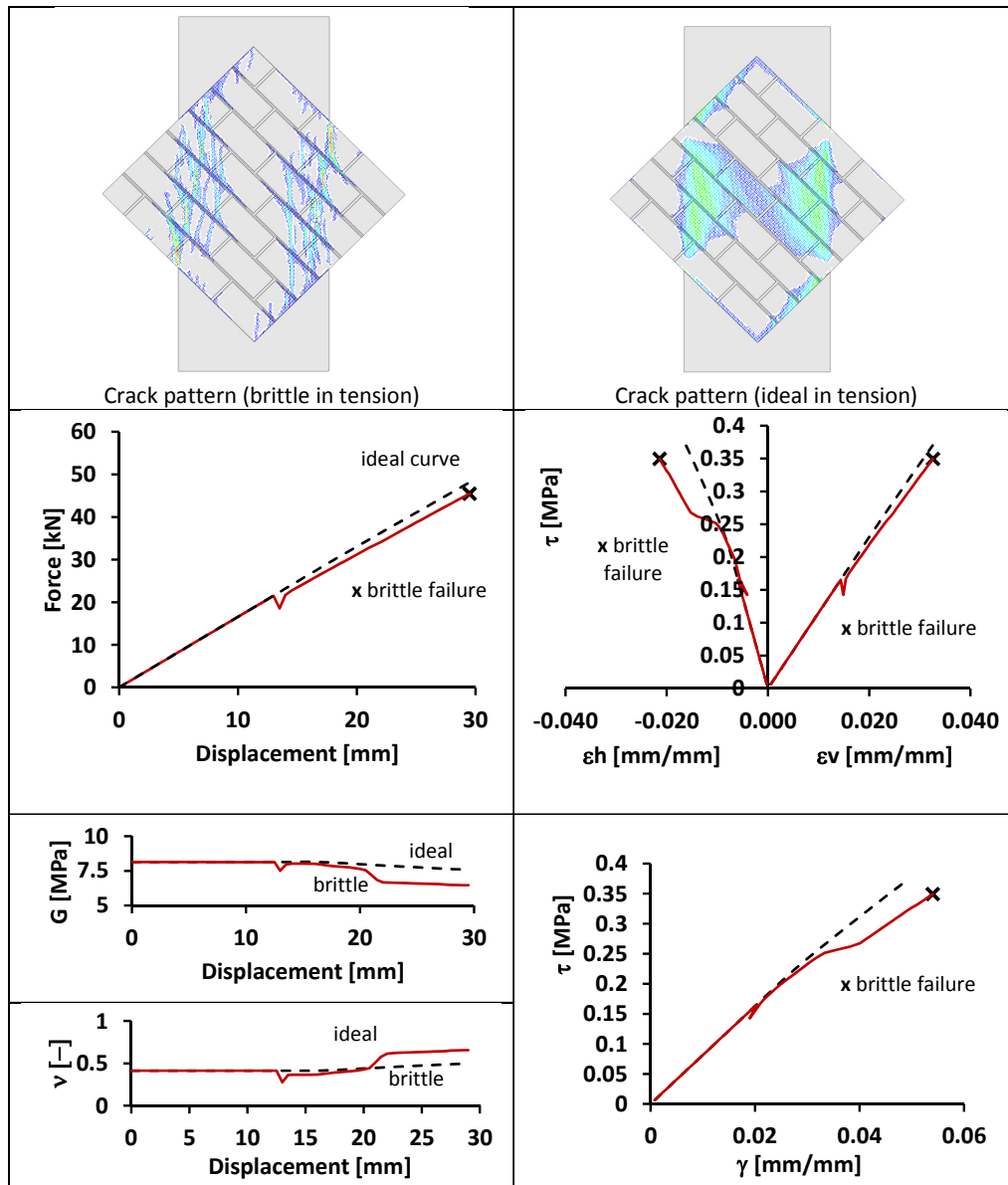


Figure 10. Numerical experimentation (reinforced MB panel).

5. Conclusions

Adobe earth constructions were copious in the ancient world. Furthermore, earth is still diffuse as a construction material, especially for its cheapness. Many historic structures, built for thousands of years, are now in need of conservation. In spite of their diffusion, only a few experimental tests are available. Actually, the variability of soil mechanic properties due to aging and composition strongly influence the seismic performance of adobe constructions. Plaster fiberglass mesh reinforcement represents a valid seismic reinforcement system for adobe building. The basic concept of this reinforcement is to improve the frictional resistance at the horizontal mortar joint location. In fact, the link between the brick units is the weakest section in the structural behavior of adobe walls. Numerical experimentation is a feasible way to deepen the knowledge of the seismic behavior of such structures. After validating the numerical model, FEM simulations can be used as a tool to increase the knowledge of the effect of fiberglass mesh reinforcement, when varying the constituent materials, on

global structural performances. The main scope of the present study is to highlight the influence of different mortar and brick compositions and aging combined with a fiberglass mesh reinforcement on the in-plane shear performance of adobe walls. A literature survey clarified the effect of curing time on the strength of the soil material, namely an increase of strength both in tension and in compression. Then, numerical analyses allowed for us to remark on the following effects. The crack pattern is directly affected by an increase of the mortar strength; in fact, a stronger mortar is able to spread the smeared cracking strain field. In Table 3, ratios are evaluated in relation to the test on the unreinforced plain soil panel. The increase of the mortar strength (e.g., equal for both LTC and MB simulations), yet having the same stiffness of basic materials, leads to an increase of global shear strength. However the increase, at a global level (about 2.5 times), is nearly proportional to the mortar strength increase at the local level (about 2.5 times), but it is mitigated by the reduction of brick strength; in fact, a reduction of the brick strength of about 20% corresponds almost proportionally to a 20% reduction of the global shear strength. However, the presence of the fiberglass mesh reinforcement makes less evident the influence of the better mechanical properties of the mortar or bricks. The mesh is able to increase the shear strength of the panel, not altering its global stiffness. An interesting future development of this research (which is based on the reinforcement of adobe during construction) could be the extension of the study to the strengthening of existing structures by means of joint external repointing. In fact, the joint's reinforcement was proven to be effectively improving the adobe shear behavior.

Table 3. The main numerical outcomes (the ratios are related to the unreinforced plain panel).

FEM model	Material level (input data)		Global level (outcomes)		
	Brick strength ratio	Mortar strength ratio	G (MPa)	τ (MPa)	τ ratio
Plain (unreinforced)	1	1	9.17	0.15	1.00
Plain (reinforced)	1	1	8.14	0.19	1.26
LTC (unreinforced)	1.25	2.5	9.17	0.32	2.20
LTC (reinforced)	1.25	2.5	8.14	0.35	2.31
MB (unreinforced)	1	2.5	9.17	0.25	1.70
MB (reinforced)	1	2.5	8.14	0.34	2.31

Acknowledgments

The analyses were developed within the activities of Rete dei Laboratori Universitari di Ingegneria Sismica—ReLUIIS for the research program funded by the Dipartimento di Protezione Civile—Progetto Esecutivo 2010–2013.

Conflicts of Interest

The authors declare no conflict of interest.

References

1. Revuelta-Acosta, J.D.; Garcia-Diaz, A.; Soto-Zarazua, G.M.; Rico-Garcia, E. Adobe as a sustainable material: A thermal performance. *J. Appl. Sci.* **2010**, *10*, 2211–2216.

2. Binici, H.; Aksogan, O.; Bakbak, D.; Kaplan, H.; Isik, B. Sound insulation of fibre reinforced mud brick walls. *Constr. Build. Mater.* **2009**, *23*, 1035–1041.
3. Houben, H.; Guillaud, H. *Earth Construction a Comprehensive Guide*; Intermediate Technology Publications: London, UK, 1994.
4. Tolles, L.E.; Krawinkler, H. *Seismic Studies on Small-Scale Models on Adobe Houses*. The John A. Blume Earthquake Engineering Center, Department of Civil Engineering, Stanford University: Stanford, CA, USA, 1990.
5. *Standard Test Method for Diagonal Tension (Shear) in Masonry Assemblages*, ASTM E519-02; American Society for Testing Materials (ASTM): West Conshohocken, PA, USA, 1981.
6. Lignola, G.P.; Prota, A.; Manfredi, G. Nonlinear analyses of tuff masonry walls strengthened with cementitious matrix-grid composites. *J. Compos. Constr.* **2009**, *13*, 243–251.
7. Turanli, L.; Saritas, A. Strengthening the structural behavior of adobe walls through the use of plaster reinforcement mesh. *Constr. Build. Mater.* **2001**, *25*, 1747–1752.
8. Turanli, L. Evaluation of Some Physical and Mechanical Properties of Plain and Stabilized Adobe Blocks. Master's Thesis, Middle East Technical University, Ankara, Turkey, 1985.
9. Manie, J.; Kikstra, W.P. *DIANA Finite Element Analysis: User's Manual release 9.4.3*; Available online: <https://support.tnodiana.com/manuals/d943/Diana.html> (accessed on 13 February 2014).
10. Lignola, G.P.; Prota, A.; Manfredi, G. Numerical investigation on the influence of FRP retrofit layout and geometry on the in-plane behavior of masonry walls. *J. Compos. Constr.* **2012**, *16*, 712–723.
11. Parisi, F.; Lignola, G.P.; Augenti, N.; Prota, A.; Manfredi, G. Rocking response assessment of in-plane laterally-loaded masonry walls with openings. *Eng. Struct.* **2013**, *56*, 1234–1248.
12. Parisi, F.; Lignola, G.P.; Augenti, N.; Prota, A.; Manfredi, G. Nonlinear behavior of a masonry sub-assembly before and after strengthening with inorganic matrix-grid composites. *J. Compos. Constr.* **2011**, *15*, 821–832.